Life Medicine

Article

Secretagogin regulates asynchronous and spontaneous glutamate release in hippocampal neurons through interaction with Doc2α

Yingfeng Tu[1,2,*,‡], Jiao Qin[1,3,‡], Qiao-Ming Zhang[2,‡], Tie-Shan Tang[4], Lifang Wang[5], Jun Yao[2,*]

[1]Key Laboratory of Birth Defects and Related Diseases of Women and Children, Department of Paediatrics, West China Second University Hospital, State Key Laboratory of Biotherapy, Sichuan University, Chengdu 610041, China
[2]State Key Laboratory of Membrane Biology, Tsinghua-Peking Center for Life Sciences, IDG/McGovern Institute for Brain Research, School of Life Sciences, Tsinghua University, Beijing 100084, China
[3]Present address: Human Sperm Bank, Key Laboratory of Birth Defects and Related Diseases of Women and Children, West China Second University Hospital, Sichuan University, Chengdu 610041, China
[4]State Key Laboratory of Membrane Biology, Institute of Zoology, Chinese Academy of Sciences, Beijing Institute for Stem Cell and Regenerative Medicine, University of Chinese Academy of Sciences, Beijing 100049, China
[5]Peking University Institute of Mental Health, NHC Key Laboratory of Mental Health, National Clinical Research Center for Mental Disorders, Peking University Sixth Hospital, Beijing 100191, China
[‡]These authors contributed equally to this work.
*Correspondence: tuyingfeng2haha@sina.com (Y.T.), jyao@mail.tsinghua.edu.cn (J.Y.)
Received: 25 August 2023; Accepted: 13 November 2023.
https://doi.org/10.1093/lifemedi/lnad041

Keywords: secretagogin; Doc2α; glutamate release; synaptic vesicle; exocytosis

Synaptic vesicle (SV) exocytosis is orchestrated by protein machineries consisting of the SNARE complex, Ca^{2+} sensors, and their partners. Secretagogin (SCGN) is a Ca^{2+}-binding protein involved in multiple forms of vesicle secretion. Although SCGN is implicated in multiple neurological disorders, its role in SV exocytosis in neurons remains unknown. Here, using knockout and knockdown techniques, we report that SCGN could regulate the asynchronous and spontaneous forms of excitatory but not inhibitory SV exocytosis in mouse hippocampal neurons. Furthermore, SCGN functioned in glutamate release via directly interacting with Doc2α, a high-affinity Ca^{2+} sensor specific for asynchronous and spontaneous SV exocytosis. Conversely, the interaction with SCGN is also required for Doc2α to execute its Ca^{2+} sensor function in SV release. Together, our study revealed that SCGN plays an important role in asynchronous and spontaneous glutamate release through its interaction with Doc2α.

Introduction

Communication between neurons relies on accurate control of neurotransmitter release. Action potential (AP)-evoked neurotransmitter release represents the primary means of synaptic communication between neurons. Evoked release consists of two forms: a fast synchronous synaptic vesicle (SV) release that occurs within several milliseconds after an AP, and a slow asynchronous component that can persist for tens of milliseconds following an AP or even tens of seconds in response to APs [1–3]. Synchronous release is fundamental for rapid and targeted communication, whereas asynchronous release is involved in the regulation of delayed synaptic signaling, postsynaptic excitability, and neuronal network activity [4–8]. In addition to evoked release, spontaneous release, which occurs independent of APs, also plays important roles in the modulation of synaptic structure and functions, such as pre- and post-synaptic excitability, postsynaptic protein synthesis, dendritic spines, and long-term synaptic plasticity [9–12].

A compelling body of studies has provided insights into the common mechanisms for the three modes of release, revealing the involvement of the canonical SNARE proteins syntaxin-1, SNAP-25, and synaptobrevin 2/VAMP2 for the fusion events in all three modes [13, 14]. Synaptotagmin-1 (Syt1), Syt2, and Syt9 serve as Ca^{2+} sensors for the fast synchronous release, but they show different kinetic properties [15–17]. Asynchronous release is mediated by two Ca^{2+} sensors, including double C2 domain protein (Doc2) and Syt7 [7, 18]. Moreover, Syt1 and Doc2 have been

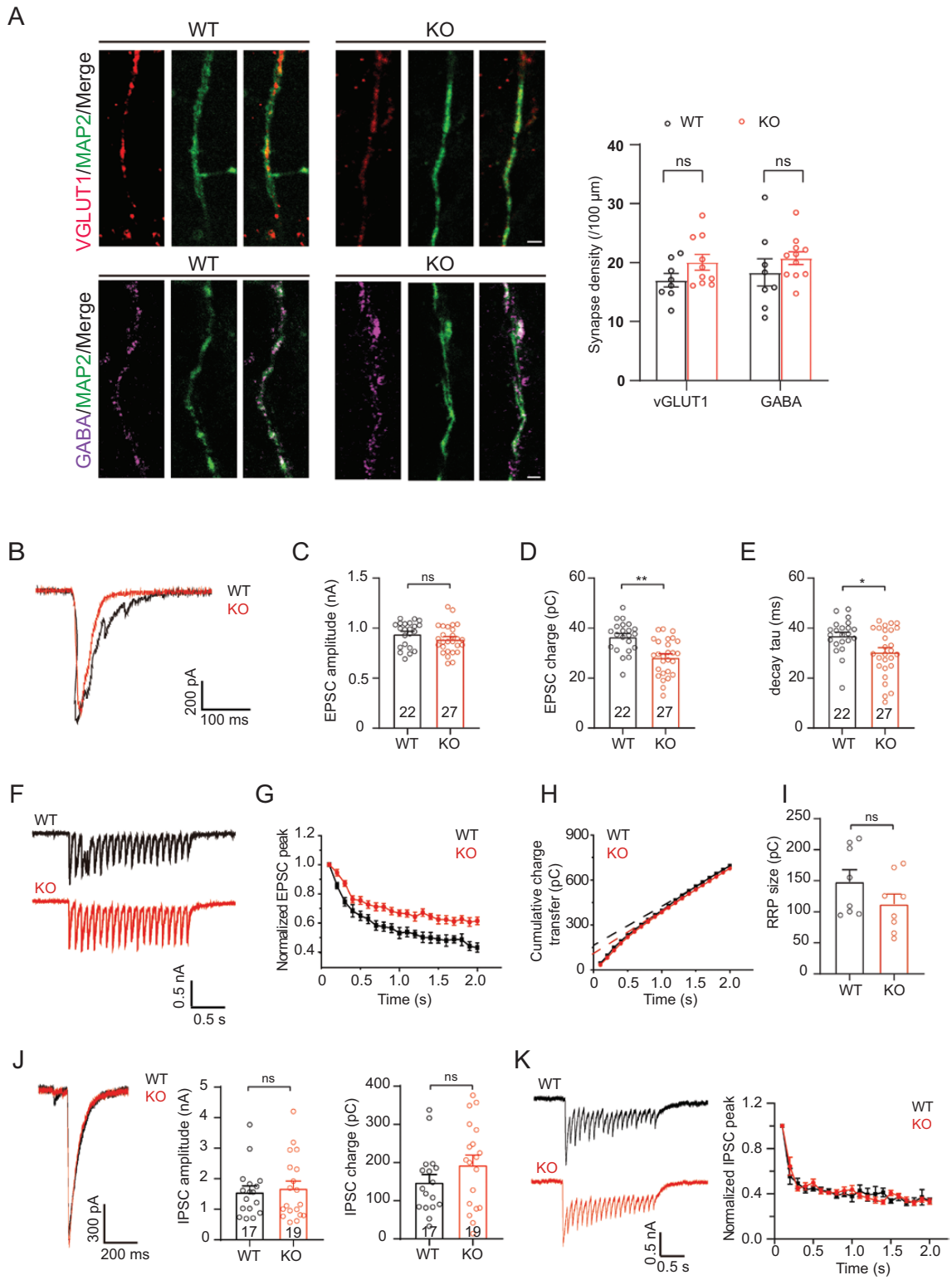

Figure 1. SCGN KO hippocampal neurons show attenuated asynchronous glutamate release.

(A) Sample immunostaining images of glutamatergic synapses and GABAergic synapses of WT and SCGN KO hippocampal neurons. Scale bar: 2 μm. Differences between groups were analyzed using two-way ANOVA. (B) Representative traces of evoked EPSCs in WT neurons or SCGN KO neurons. (C–E) Bar graphs summarizing the amplitude (C), charge transfer over 0.5 s (D), and decay tau (E) of evoked EPSCs recorded from WT neurons and SCGN KO neurons. (F) Representative EPSC traces evoked by 20 action potentials at 10 Hz in WT neurons and SCGN KO neurons. (C) Summary of normalized peak of EPSCs during train stimulation. (H) Cumulative charge transfer of EPSCs evoked by train stimulation. (I) Bar graph showing the RRP size measured by extrapolating the cumulative charge transfer curve. (J) Sample traces

reported to regulate spontaneous release [19, 20]. Syt and Doc2 proteins all have two conserved C2 domains (C2A and C2B). While Syt1 is attached to the SVs by its transmembrane domain, Syt7 is localized in the presynaptic plasma membrane and Doc2 is cytosolic and soluble [21–24]. Doc2 proteins (including Doc2α and Doc2β) function *in vitro* on timescales consistent with residual Ca^{2+}-triggered release, whereas Syt1 only responds to bulk Ca^{2+} [25]. It has been suggested that Doc2α and Doc2β function as Ca^{2+} sensors for excitatory and inhibitory spontaneous release, respectively, due to the distinct expression patterns of the two isoforms [26]. However, there is a report against the role of Doc2 as a Ca^{2+} sensor for neurotransmitter release [27].

Secretagogin (SCGN) is a Ca^{2+} binding protein comprised of six EF-hands [28, 29]. SCGN is highly expressed in neuroendocrine cells, including pancreatic β cells, enteroendocrine cells, and certain types of neurons. Depletion of SCGN in pancreatic β cells causes a significant reduction of glucose-stimulated insulin secretion; accordingly, SCGN knockout (KO) mice display reduced insulin production and glucose intolerance [28, 30–32]. In the brain, SCGN is highly enriched in the hippocampus of humans and mice, the cerebellum of humans, and the olfactory bulb of mice, and SCGN deficiency might be involved in the pathogenesis of various neurological disorders, including autism, schizophrenia, and neurodegeneration, in addition to inflammatory bowel disease [33–40]. SCGN is known to mediate the secretion of matrix metalloprotease-2 (MMP2) and corticotropin-releasing hormone (CRH) in the central nervous system (CNS) [32, 37, 41], likely through cooperating with the SNARE complex. Recently, we have determined the crystal structure of SCGN in a complex with the SNAP-25 fragment SNAP-25-J (143–170 aa) [42]. We have also shown that SCGN controls neuronal growth and brain development in zebrafish, likely via interacting with SNAP-25 or its close homolog, SNAP-23 [42]. Recently, it has been found that SCGN and Doc2α cooperate to promote the development of the mouse brain. Both SCGN KO mice and Doc2α KO mice can show neurodevelopmental abnormalities, defective neural activity, as well as social and repetitive behavioral deficits [43]. However, it remains elusive whether SCGN plays a direct role in neurotransmitter release and the possible mechanisms are unexplored.

In this study, given the essential role of Doc2α in neurotransmitter release and the interaction of SCGN/Doc2α, we investigated the functions of SCGN in SV exocytosis via patch-clamp recording analyses of cultured hippocampal neurons. We found that SCGN was required for asynchronous and spontaneous glutamate release but not for inhibitory GABAergic neurotransmission. SCGN directly interacted with the linker between the C2A and C2B domains of Doc2α but not Doc2β. The direct interaction between SCGN and Doc2α was critical for both proteins to function in excitatory neurotransmission. We concluded that SCGN and Doc2α cooperate in the regulation of asynchronous release and spontaneous excitatory SV release in mouse hippocampal neurons.

Results

SCGN KO hippocampal neurons show attenuated asynchronous glutamate release

To examine the roles of SCGN in SV exocytosis, we first investigated the synapse density in 14–17 days *in vitro* (DIV) cultured hippocampal neurons of the SCGN KO mice. We used vGLUT1 as a presynaptic marker for excitatory glutamatergic neurons and GABA as a presynaptic marker for inhibitory GABAergic neurons. The results showed that the SCGN KO and wild-type (WT) neurons showed a similar density of presynaptic boutons (Fig. 1A). Then, we investigated the AP-evoked AMPA receptor (AMPAR)-mediated excitatory postsynaptic currents (EPSCs) in the SCGN KO hippocampal neurons (Fig. 1B). Analysis of EPSCs evoked by single APs revealed that compared with the WT control group, the SCGN KO neurons did not show any significant changes in the amplitude of EPSCs (Fig. 1C); however, we observed a decreased total charge transfer and a faster decay rate of the EPSCs in the SCGN KO neurons (Fig. 1D and 1E), indicating that SCGN could probably modulate asynchronous glutamate release. It has been widely reported that attenuation of asynchronous release often resulted in a slower depression of EPSC amplitude during high-frequency train stimulation [44], possibly because more vesicles were rendered for synchronous release. We thus examined the kinetics of EPSCs during a 2-s 10 Hz train stimulation in the SCGN KO neurons (Fig. 1F). Compared with the WT control, the SCGN KO neurons exhibited a slower depression of EPSC amplitude (Fig. 1G), which is consistent with the attenuated asynchronous release. We also estimated the readily releasable pool (RRP) size by extrapolating the cumulative charge transfer during the train stimulation (Fig. 1H). The results indicated that the RRP size was unchanged in the SCGN KO neurons (Fig. 1I).

Next, we investigated the AP-evoked inhibitory PSCs (IPSCs) in the SCGN KO hippocampal neurons. We found that the single AP-evoked IPSCs failed to show any significant differences in the amplitude or charge transfer between the WT control and SCGN KO neurons (Fig. 1J). Moreover, analysis of train APs-evoked IPSCs revealed that the two groups of neurons showed similar depression rates of IPSCs (Fig. 1K). These results are

(left) and quantification for the amplitude (middle) and charge transfer (right) of evoked IPSCs recorded in WT and KO neurons. (K) Sample traces (left) and normalized amplitude depression (right) of IPSCs evoked by 2-s 10 Hz stimulation in WT and KO neurons. Data are presented as mean ± standard error for the mean (SEM). *P < 0.05; **P < 0.001; error bars, SEM. ns, not significant.

consistent with our previous report that SCGN was not enriched in GABAergic interneurons [43].

Together, the results of the analysis of evoked EPSCs/IPSCs in the SCGN KO neurons indicated that SCGN was required for the asynchronous phase of glutamate release but not for the GABA release.

SCGN KD attenuates asynchronous glutamate release in hippocampal neurons

To avoid any developmental disturbance in the KO mice, we applied the short hairpin RNA (shRNA)-based gene knockdown technique to suppress *SCGN* expression in WT-cultured hippocampal neurons. Analysis of single AP-evoked EPSCs revealed that compared with the WT neurons expressing a scrambled shRNA, the SCGN KD neurons did not show any significant difference in the EPSC amplitude, but they showed a significantly reduced total charge transfer and a faster decay time constant of EPSCs (Fig. 2A–D). Furthermore, we measured the train stimulation evoked EPSCs and found that compared with the control group, the KD neurons showed a decelerated depression in the EPSC amplitude (Fig. 2E and 2F); however, the RRP size in the KD neurons was comparable to that of the control group (Fig. 2G and 2H). In addition, we analyzed the AP-evoked IPSCs in the KD neurons. The results indicated that the amplitude and charge transfer of single AP-evoked IPSCs were unaffected by the SCGN KD (Fig. 2I and 2J); the depression of train-evoked IPSCs were also unchanged by the SCGN KD (Fig. 2K and 2L).

Together, these results were similar to our observations in the SCGN KO neurons, and confirmed that SCGN played an important role in asynchronous neurotransmitter release in excitatory glutamatergic neurons but not in inhibitory GABAergic neurons.

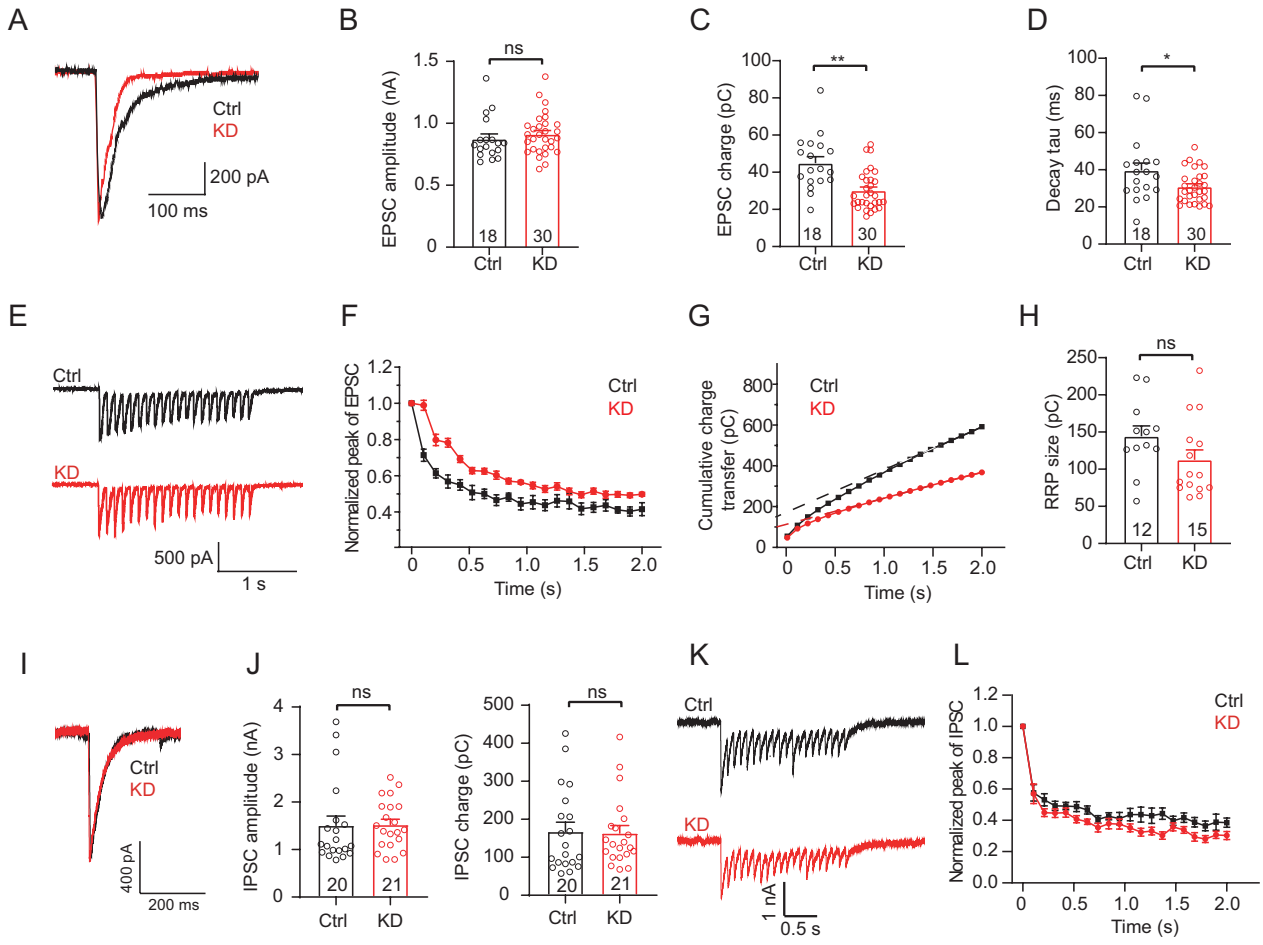

Figure 2. SCGN KD results in compromised asynchronous glutamate release.

(A) Representative traces of evoked EPSCs in WT neurons expressing SCGN shRNA or a scrambled shRNA. (B–D) Bar graphs summarizing the amplitude (B), charge transfer (C), and decay tau (D) of EPSCs. (E) Representative EPSC traces evoked by 20 action potentials at 10 Hz in scrambled and SCGN KD neurons. (F) Summary of normalized peak of EPSCs during train stimulation. (G, H) Cumulative charge transfer (G) of EPSCs and RRP size (H) measured by extrapolating the cumulative charge transfer curve. (I) Sample traces of evoked IPSCs recorded in scrambled control and SCGN KD neurons. (J) Quantitative analysis of the amplitude (left) and charge transfer (right) of evoked IPSCs. (K, L) Sample traces (K) and normalized amplitude depression (L) of IPSCs evoked by 2-s 10 Hz stimulation in scrambled control and SCGN KD neurons. *P < 0.05; **P < 0.001; error bars, SEM. ns, not significant.

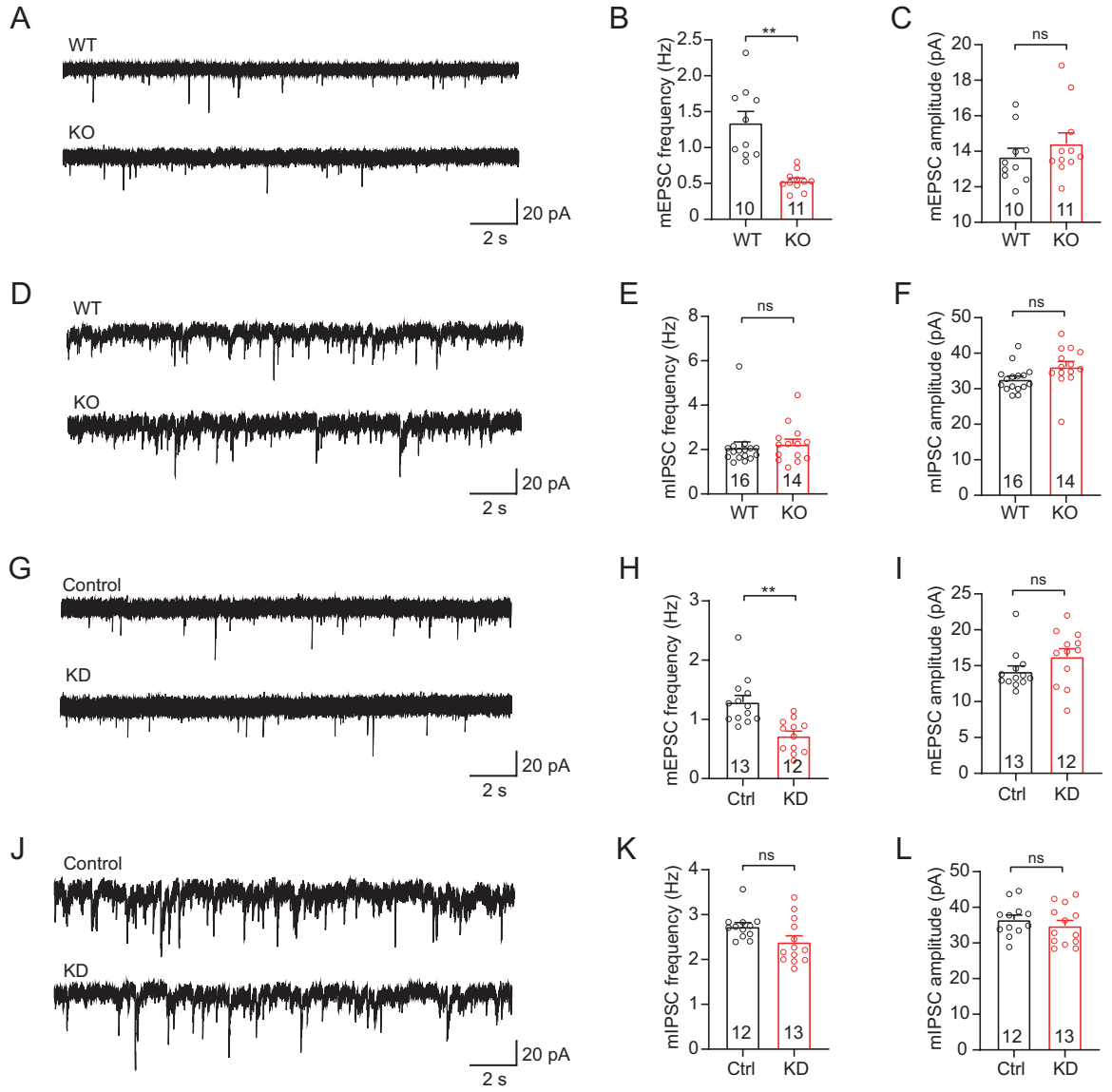

Figure 3. SCGN contributes to spontaneous glutamate release.

(A) Sample traces of mEPSCs recorded from WT and SCGN KO hippocampal neurons. (B, C) Quantitative analysis of mEPSC frequency (B) and amplitude (C) in WT and SCGN KO neurons. (D–F) Sample traces (D) and quantification (E, F) indicating that the amplitude and frequency of mIPSCs in SCGN KO neurons were comparable to WT neurons. (G–I) Sample mEPSC traces (G), and quantification of mEPSC frequency (H) and amplitudes (I) in WT scrambled control and SCGN KD neurons. (J–L) Representative traces (J) and quantification (K, L) indicating that mIPSCs were unchanged in SCGN KD neurons. *$P < 0.05$; **$P < 0.001$; error bars, SEM. ns, not significant.

SCGN can regulate excitatory spontaneous release

We then investigated whether SCGN plays a role in AP-independent spontaneous SV release. To this end, we recorded miniature EPSCs (mEPSCs) in the SCGN KO hippocampal neurons (Fig. 3A). We observed that compared with the WT control, the SCGN KO neurons showed a decreased mEPSC frequency (Fig. 3B), but the mEPSC amplitude was unaffected (Fig. 3C). We also analyzed the decay time of mEPSCs and found that SCGN KO did not significantly change the mEPSC decay time (Fig. S1A). These results indicated that SCGN played an important role in spontaneous glutamate release in hippocampal neurons, whereas the postsynaptic AMPARs were unaffected. Next, we investigated the miniature IPSCs (mIPSCs) in the hippocampal neurons (Fig. 3D). We found that compared with the WT control, the SCGN KO neurons did not show any significant changes in either mIPSC frequency or amplitude (Fig. 3E and 3F). Hence, the SCGN deficiency probably led to deficits specifically in glutamatergic but not GABAergic spontaneous SV exocytosis.

We also investigated the hippocampal neurons with SCGN KD. The results indicated that compared with the scramble control group, the mEPSC frequency was significantly reduced in the KD neurons, while the mEPSC amplitude and decay time were unchanged (Figs. 3G–I, S1B). Moreover, analysis of mIPSCs revealed that both the frequency and the amplitude of mIPSCs

were similar between the KD and scramble neurons (Fig. 3J–L). These results are consistent with our observations in the SCGN KO neurons, and further supported an important role of SCGN in spontaneous glutamate release.

Together, our results of SCGN KO and KD both indicated that SCGN contributed to excitatory but not inhibitory spontaneous release in mouse hippocampal neurons.

SCGN directly and specifically interacts with Doc2α

Previously, we have observed in cultured neurons that SCGN can directly bind to the linker between the C2A and C2B domain of Doc2α but not that of Doc2β [43]. To further verify this finding, we performed GST pull-down assays using purified proteins. Consistent with our previous observations, the results showed that the C2A–C2B linker region was sufficient and necessary for the association between Doc2α and SCGN (Fig. 4A and 4B). The linker region of Doc2α is evolutionarily conserved among the Doc2α homologs; moreover, it is unique among the Doc2/Synaptotagmin family (Fig. S2), indicating that the interaction with SCGN is likely unique for Doc2α.

The recently determined crystal structure of SCGN in the complex with a SNAP-25-J has revealed that SNAP-25 adopted a helical structure and bound to EF-hands 5 and 6 of SCGN [42]. Interestingly, the linker of Doc2α has also been predicted

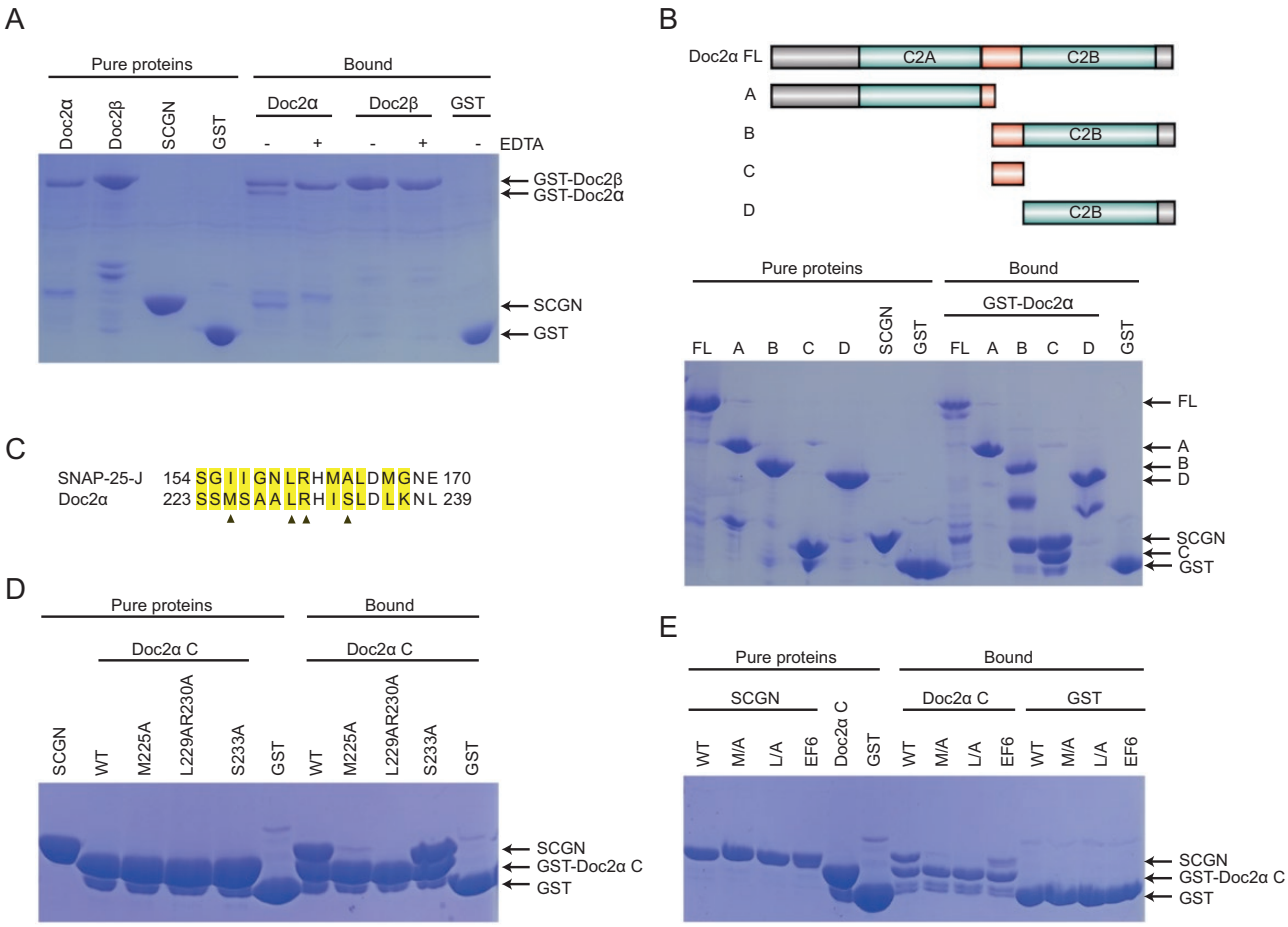

Figure 4. SCGN and Doc2α interact in a Ca^{2+}-dependent manner.

(A) Coomassie blue-stained SDS–PAGE gels of GST pull-down assays performed with GST-human Doc2α, GST-human Doc2β or GST, and purified SCGN, in the presence or absence of 2 mM $CaCl_2$. (B) Doc2α interacts with SCGN through its linker region. Upper, schematic representation of the Doc2α fragments used in pull-down assay. The linker region is shown in pink. Lower, a sample Coomassie blue-stained SDS–PAGE gel of GST pull-down assays performed with GST-Doc2α full-length (FL), fragments or GST, and purified SCGN, in the presence of 2 mM $CaCl_2$. (C) Sequence alignment of the Doc2α linker region and the SCGN-contacting SNAP-25-J. Yellow background highlights SCGN-interacting residues in SNAP-25 or the corresponding residues in Doc2α. (D) GST pull-down assays performed with GST-Doc2α C fragment WT or mutants, or GST, and purified SCGN protein, in the presence of 2 mM $CaCl_2$. After incubation with soluble proteins, the resin was extensively washed. The resin-bound proteins were then subjected to SDS-PAGE and Coomassie blue staining. (E) A sample Coomassie blue-stained SDS–PAGE gel of GST pull-down assays performed with GST-human Doc2α C fragment, or GST, and purified SCGN wild-type (WT) or mutants, in the presence of 2 mM $CaCl_2$, to identify SCGN residues critical for interaction with Doc2α. EF6: alanine substitution of the first and third positions of the loop in the sixth EF of SCGN (D254A/N256A).

to adopt an α-helical structure, which is similar to the SNAP-25-J in the crystal structure. Furthermore, amino acids within the Doc2α linker displayed a remarkable similarity with that of the SNAP-25-J that contacting SCGN (Fig. 4C). Consistent with our prediction, mutations of multiple conserved residues in Doc2α, M225A, or L229A/R230A, nearly completely abolished the interaction of Doc2α with SCGN (Fig. 4D). SCGN interacted with SNAP-25 mainly through hydrophobic interactions, and multiple hydrophobic residues of SCGN, including M230 and L232, were critical for the interaction between SCGN and SNAP-25 (Fig. S3A). Similarly, the M230A and L232A mutants of SCGN, as well as the mutations of the Ca^{2+} binding sites in EF6 (D254A/N256A), could also abolish the binding of SCGN to Doc2α (Fig. 4E), indicating that Doc2α and SNAP-25 could bind to the same site of SCGN. Using isothermal titration calorimetry (ITC) assays, we determined the binding affinity between SCGN and Doc2α or SNAP-25 in the presence of Ca^{2+}. Whereas the SNAP-25-J bound to human SCGN with a dissociation constant ~280 nM, which is similar to our previous measurement [42], Doc2α showed a slightly higher binding affinity (K_d ~90 nM) to SCGN (Fig. S3B). Finally, Doc2α inhibited the binding of GST-SNAP-25-J to SCGN in a dose-dependent manner (Fig. S3C). Taken together, our results indicated that Doc2α directly interacted with SCGN, and Doc2α and SNAP-25 likely bound to the same motif of SCGN.

SCGN regulates glutamate release through its Doc2α/SNAP-25 binding motif

To test whether SCGN functioned in asynchronous and spontaneous glutamate release through its Doc2α/SNAP-25 binding motif, we re-introduced WT full-length SCGN ($SCGN^{FL}$) or two SCGN mutants defective in association with Doc2α or SNAP-25 ($SCGN^{M230A/L232A}$ or $SCGN^{EF6}$), into the hippocampal neurons of the SCGN KO mice. We observed that re-introduction of $SCGN^{FL}$ into the KO neurons could rescue the compromised decay kinetics and charge transfer of single AP-evoked EPSCs; however, expression of $SCGN^{M230A/L232A}$ or $SCGN^{EF6}$ failed to restore the defective EPSCs (Fig. 5A–D). Moreover, analysis of train stimulation evoked EPSCs revealed that while expressing the $SCGN^{FL}$ in the KO neurons could rescue the delayed depression of EPSC amplitude, the SCGN mutants failed to induce any significant changes (Fig. 5E and 5F). These results suggested that the Doc2α/SNAP-25 binding motif probably played an important role in SCGN-mediated asynchronous glutamate release.

We next examined whether SCGN regulated spontaneous excitatory SV release through its Doc2α/SNAP-25 binding motif (Fig. 5G). Lentiviral introduction of $SCGN^{FL}$ into the KO neurons could rescue the reduced mEPSC frequency; however, neither $SCGN^{M230A/L232A}$ nor $SCGN^{EF6}$ could support spontaneous SV release as efficiently as $SCGN^{FL}$ did (Fig. 5H). These results are consistent with our observations in evoked SV release. Moreover, all groups of neurons showed similar levels of mEPSC amplitude (Fig. 5I). In a complementary overexpression experiment to compare excitatory and inhibitory spontaneous SV release, we observed that overexpressing $SCGN^{FL}$ but not $SCGN^{M230A/L232A}$ or $SCGN^{EF6}$ in WT hippocampal neurons could significantly increase the mEPSC frequency, without affecting the amplitude of the mEPSCs (Fig. S4A–C); in contrast, overexpression of $SCGN^{FL}$ failed to affect either the frequency or the amplitude of the mIPSCs (Fig. S4D–F). These results further supported that the Doc2α/SNAP-25 binding motif of SCGN was required for the excitatory but not inhibitory spontaneous SV exocytosis.

Together, our results indicated that SCGN regulated asynchronous and spontaneous glutamate release through its Doc2α/SNAP-25 binding motif.

Doc2α functions in glutamate release through its interaction with SCGN.

As Doc2α is known to regulate asynchronous and spontaneous SV release and Doc2α contributes to neurodevelopment through interacting with SCGN, we next determined whether Doc2α-triggered SV release requires its interaction with SCGN. Previously, it has been suggested that in cultured hippocampal neurons, Doc2 deficiency could not affect the density of synapses [27], which was verified by our immunostaining analysis in cultured Doc2α KD hippocampal neurons (Fig. S5A). To test the role of SCGN–Doc2α interaction, we designed Doc2α mutants in which the SCGN-binding linker was replaced with either a nine-residue linker (GGSGGSGGS) (termed $Doc2α^{del\text{-}linker}$) or the linker of Doc2β ($Doc2α^{chimera}$) (Fig. S5B). Analysis of single AP-evoked EPSCs revealed that Doc2α KD did not alter the amplitude of EPSCs, but led to a significantly decreased EPSC charge transfer compared with the WT neurons (Fig. 6A–C). This result is consistent with our previous findings that Doc2α KD resulted in a compromised asynchronous SV release [7]. Furthermore, the defects in EPSCs in the KD neurons could be rescued by re-introduction of WT full-length Doc2α ($Doc2α^{FL}$) but not by $Doc2α^{del\text{-}linker}$ or $Doc2α^{chimera}$ (Fig. 6B and 6C). We also investigated the train stimulation evoked EPSCs (Fig. 6D). The results indicated that the Doc2α KD neurons showed a decelerated EPSC depression during the train stimulation, which is consistent with our previous findings [7]. Furthermore, expression of $Doc2α^{FL}$ but neither mutant in Doc2α KD neurons could restore the EPSCs (Fig. 6E). Hence, the interaction with SCGN was required for Doc2α to function in asynchronous glutamate release.

We next determined whether interacting with SCGN was important for Doc2α to function in the spontaneous SV release (Fig. 6F). Consistent with previous studies [26], Doc2α KD induced a significant decrease in the mEPSC frequency without altering the mEPSC amplitude compared with the scrambled control (Fig. 6G and 6H). Moreover, expression of $Doc2α^{FL}$ in the Doc2α KD neurons could largely restore the mEPSC frequency, whereas KD neurons expressing $Doc2α^{del\text{-}linker}$ or $Doc2α^{chimera}$ failed to induce

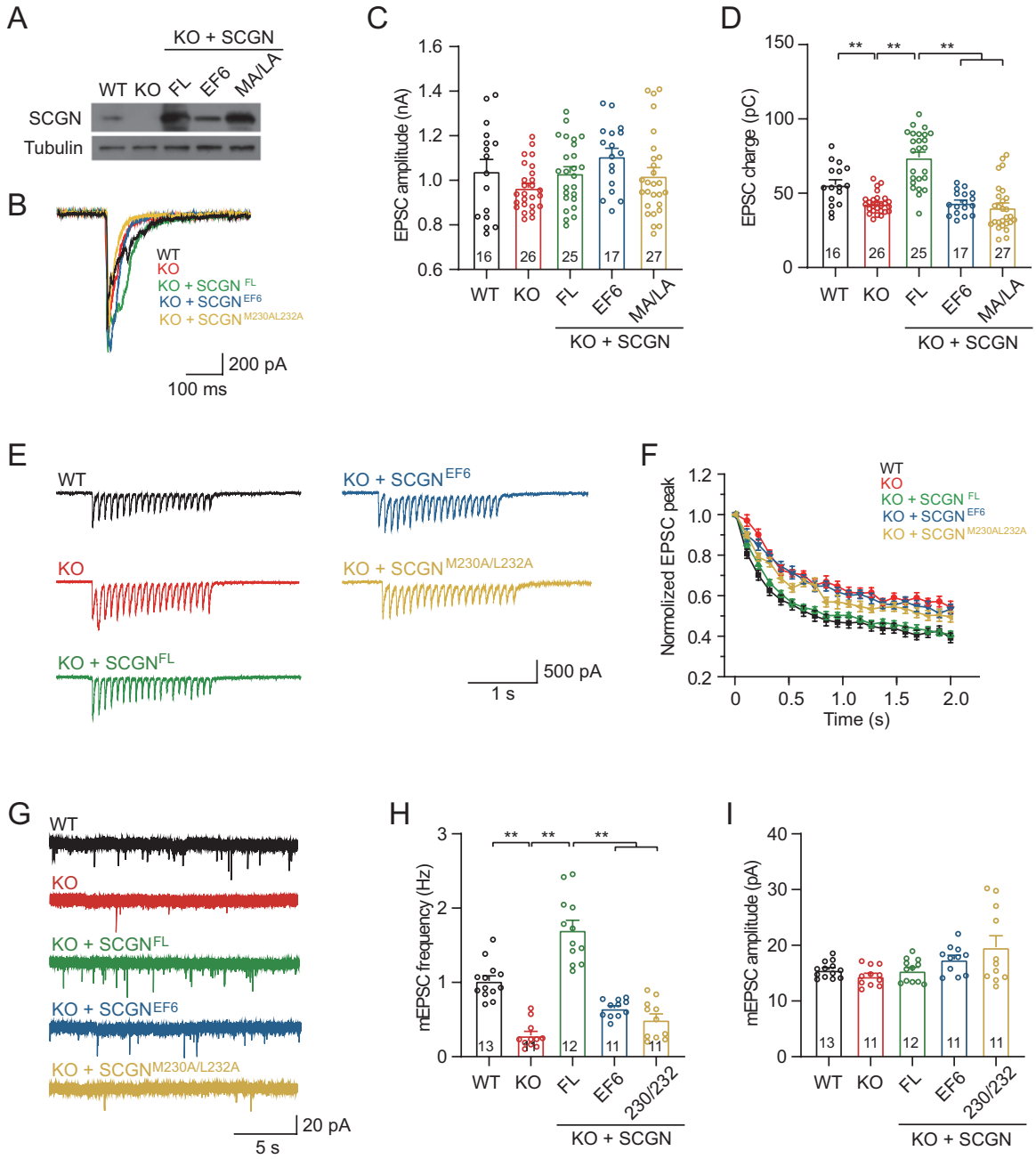

Figure 5. SCGN functions in excitatory neurotransmission through interacting with Doc2α.

(A) Immunoblot analysis of SCGN protein level in WT neurons, SCGN KO neurons, and KO neurons expressing SCGN^{FL}, SCGN^{EF6}, or SCGN$^{M230A/L232A}$. (B) Representative traces of evoked EPSCs in WT neurons, SCGN KO neurons, and KO neurons expressing SCGN^{FL} or mutants. (C, D) Summary of the amplitude (C) and charge transfer (D) of EPSCs. (E, F) Representative traces (E) and amplitude depression (F) of EPSCs evoked by 20 action potentials at 10 Hz in WT neurons, SCGN KO neurons, and KO neurons expressing SCGN^{FL} or mutants. (G) Sample traces of mEPSC recorded from WT neurons, SCGN KO neurons, and KO neurons expressing SCGN^{FL} or mutants. (H, I) Summary of the frequency (H) and amplitude (I) of mEPSC. *P < 0.05; **P < 0.001; error bars, SEM. ns, not significant.

any significant changes (Fig. 6G and 6H). These results indicated that interaction with SCGN was required for Doc2α to function in spontaneous glutamate release.

In summary, our results indicated that interaction with SCGN was required for Doc2α to execute its Ca^{2+} sensor functions in asynchronous and spontaneous glutamate release.

Discussion

As asynchronous release and spontaneous release are mediated by residual Ca^{2+} and high-affinity Ca^{2+} sensors, they might share some regulatory elements and functional components. For instance, Doc2α has been suggested to function in both spontaneous and asynchronous glutamate release [7, 20, 27].

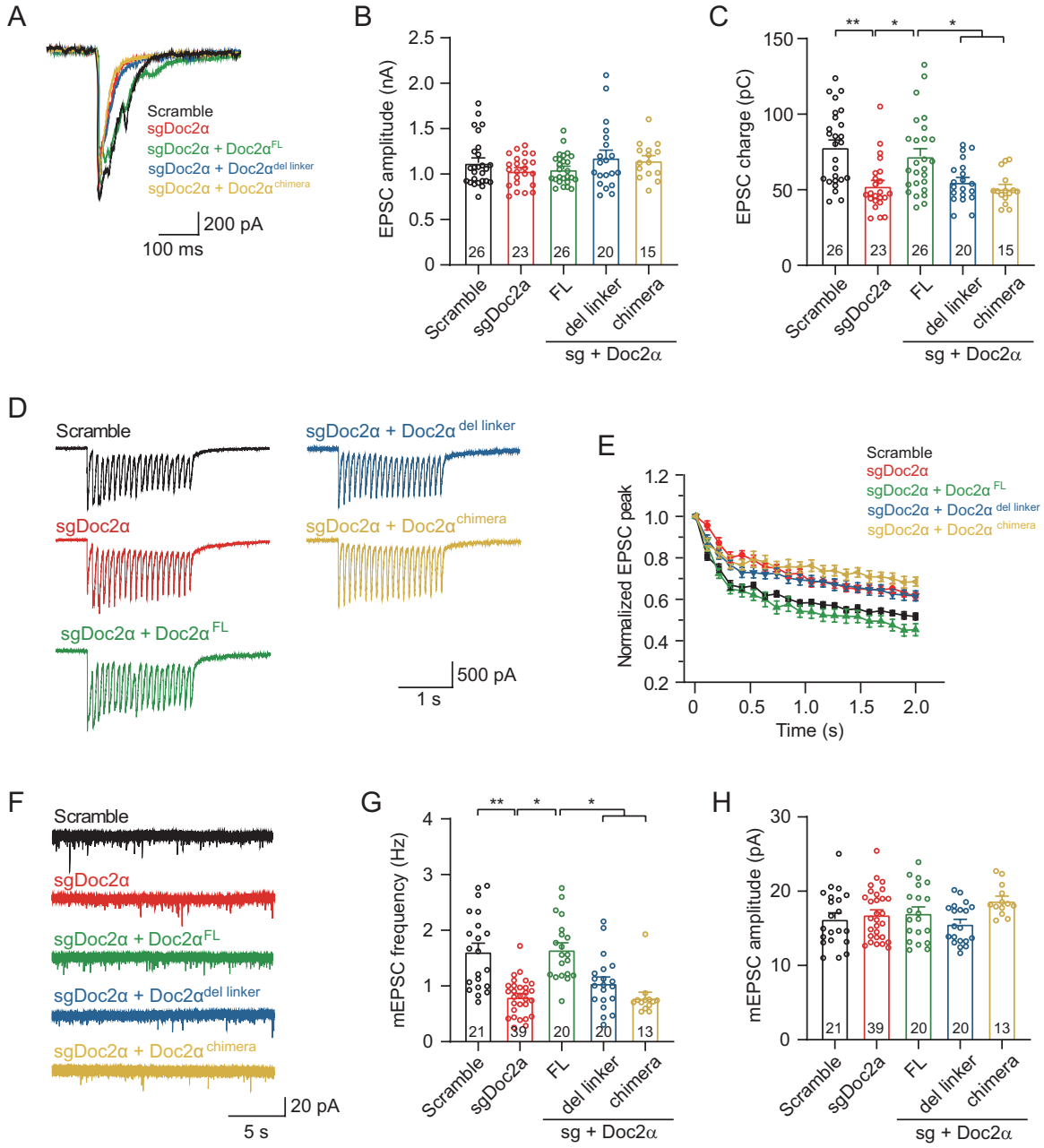

Figure 6. Interaction with SCGN is required for Doc2α to function in excitatory SV release.

(A) Representative traces of evoked EPSCs recorded in WT neurons, Doc2α KD neurons, and KD neurons expressing Doc2α^{FL}, Doc2α$^{Del\text{-}linker}$, or Doc2α^{chimera}. (B, C) Bar graphs summarizing the amplitude (B) and charge transfer (C) of evoked EPSC recorded in WT neurons, Doc2α KD neurons, and KD neurons expressing Doc2α^{FL} or mutants. (D) Representative traces of EPSCs evoked by 20 action potentials at 10 Hz. (E) Normalized peak of train-evoked EPSCs. (F) Representative traces of mEPSCs recorded from WT neurons, Doc2α KD neurons, and KD neurons expressing Doc2α^{FL} or mutants. (G, H) Quantification of frequency (G) and amplitude (H) of mEPSCs recorded from WT neurons, Doc2α KD neurons, and KD neurons expressing Doc2α^{FL} or mutants. *P < 0.05; **P < 0.001; error bars, SEM. ns, not significant.

However, unlike the well-studied synchronous neurotransmitter release, many details regarding the mechanisms controlling asynchronous and spontaneous release have remained unclear. In the present study, we demonstrated that SCGN was a novel regulator for these two types of excitatory SV release. We observed that both the SCGN KO and KD neurons showed a faster decay rate of evoked EPSCs compared with their control groups. As the mEPSC decay time was not affected by the deletion or suppression of SCGN, these results indicated that the faster decay of evoked EPSCs resulted from an attenuation of asynchronous release but not AMPAR kinetics changes. Doc2α and Doc2β are mainly expressed in glutamatergic and

GABAergic neurons, respectively [26]. Previously, we have reported that lentiviral introduction of SCGN through a CMV promoter induced SCGN expression only in excitatory glutamatergic neurons but not in GABAergic interneurons [43]. In the present study, we observed that SCGN specifically regulated excitatory SV release while the inhibitory release remained unaffected. Importantly, both the SCGN mutants defective in binding to Doc2α and the mutation of Doc2α linker region indispensable for the SCGN-binding activity impaired Doc2α-induced neurotransmitter release, including the spontaneous and asynchronous excitatory release. Based on these results, we therefore concluded that SCGN specifically regulated excitatory, but not inhibitory, asynchronous, and spontaneous release through its interaction with Doc2α (Fig. 7).

It has been recently reported that SCGN could inhibit SNARE-mediated vesicle fusion *in vitro* through interacting with SNAP-25 [42]. As Doc2α and SNAP-25 bind to the same motif of SCGN, it is possible that Doc2α might relieve the inhibition of SCGN on SNARE-mediated vesicle fusion through a direct competition with SNAP-25, thus promoting slow vesicle fusion. This is supported by our finding that the Doc2α-binding affinity of SCGN is two to three times greater than its binding with SNAP-25 (Fig. S3B). Ideally, one would expect that retrieval of SNAP-25 following SCGN deletion would contribute to vesicle fusion. However, we did not observe any significant changes in the amplitude of single AP-evoked EPSCs in the SCGN-deficient neurons. This might be because the expression level of SNAP-25 is far beyond the quantity required for maximizing the fast synchronous release. Thus, a proportion of SNAP-25 being bound by SCGN is insufficient to influence the synchronous release. This explanation is supported by the fact that the amplitude of single AP-evoked EPSCs is not influenced by down-regulation of slow asynchronous release [7]. On the other hand, we cannot fully exclude the possibility that Doc2α and SNAP-25 bind to a subpopulation of SCGN separately, without or only with partial competition. In this case, the Doc2α- and SNAP-25-interactions of SCGN exist in parallel and show lesser crosslinking.

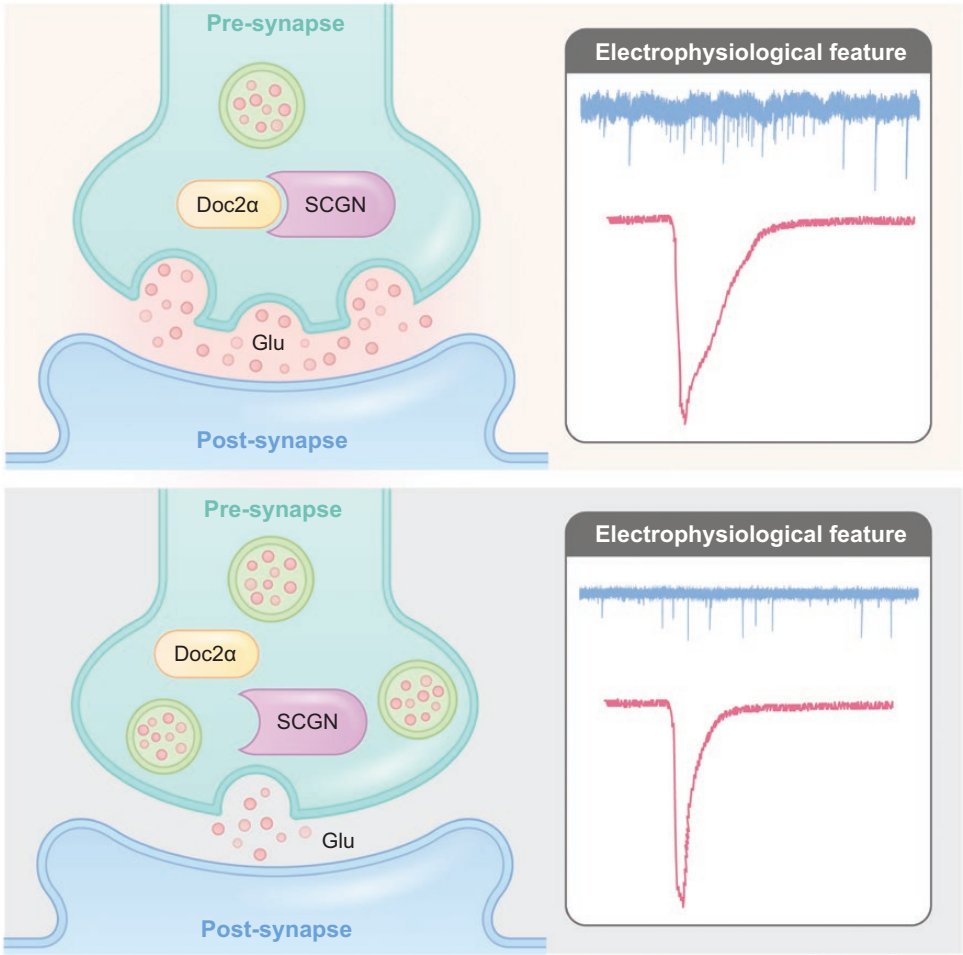

Figure 7. Graphical summary.

SCGN directly interacts with Doc2α to promote asynchronous and spontaneous glutamate release in mouse hippocampal neurons. The direct interaction between SCGN and Doc2α is crucial for both proteins to function in excitatory neurotransmission, and disrupting their interaction impairs asynchronous and spontaneous glutamate release.

Research limitations

In the present study, we employed cultured hippocampal neurons as the model to investigate the role of SCGN in asynchronous and spontaneous release. Previously, it has been found that SCGN can regulate synapse density during neurodevelopment in animals. In the neuronal culture system, SCGN deficiency failed to affect synapse density, and thus we could evaluate its effects on neurotransmitter release within a single synapse. However, it is unclear whether the results we observed in this study exist in living animals. In the future, it would be necessary to use dissected brain slices as a model to investigate the role of SCGN in asynchronous and spontaneous release.

Methods

Primary neuronal cultures

Hippocampal neurons were cultured from WT and SCGN KO mice at postnatal day 0–1. Briefly, hippocampi were dissected from mouse brain and digested for 15 min in 0.25% trypsin (Life Technologies) at 37°C. After washing with Dulbecco's modified eagle medium (DMEM) supplemented with 2% FBS, the hippocampi were mechanically dissociated and plated onto 12-mm glass coverslips coated with poly-D-lysine (Sigma). Cultures were grown in Neurobasal-A medium (Life Technologies) supplemented with 2% B27 (Life Technologies) and 2 mM Glutamax (Life Technologies) and maintained in a humidified 5% CO_2 incubator at 37°C.

Lentivirus production and infection of cultured neurons

The SCGN shRNA (sequence:5'-CCGGGTAACTTTCTTCGAGACCTTTCTCGAGAAAGGTCTCGAAGAAAGTTACTTTTTG-3') used in this study were purchased from The MISSION shRNA Library and has been verified to have a high KD efficiency [43]. HEK293FT cells were maintained in DMEM supplemented with 10% FBS, 100 U/mL streptomycin, 100 mg/mL penicillin, and 2 mM Glutamax (Life Technologies). Lentiviral particles were generated by co-transfection of virus packaging vectors (pVSVg and psPAX2) and lentiviral expression vectors. Cell transfection was performed using PEI (Polysciences) following the manufacturer's protocols. Cells were cultured in fresh DMEM for another 72 h. Virus supernatant was collected, filtered with a 0.22-μm PVDF filter (Millipore), ultracentrifuged at 25,000 rpm for 2 h, and stocked in phosphate-buffered saline (PBS), with a final volume of 100 μL. Viral particles were used to infect the neurons at 3 DIV. For rescue experiments in Doc2α KD neurons, lentivirus encoding the exogenous rescue gene was applied at 5 DIV.

Immunofluorescence

Neuronal cultures infected with lentivirus were cultured for 14–16 DIV. These neurons were washed three times with PBS and fixed with 4% paraformaldehyde (PFA) in PBS for 15 min at room temperature (RT). Following fixation, the neuronal cultures were washed three times with PBS. Neurons were then permeabilized with 0.25% Triton X-100 in PBS for 15 min at RT and blocked in blocking solution containing 0.25% Triton X-100 and 3% BSA in PBS for 1 h at RT. Primary antibodies were diluted in blocking solution and the neurons were incubated overnight at 4°C. Cultures were washed three times and then incubated with Alexa-conjugated secondary antibodies in blocking solution for 2 h at RT. Following three washes, coverslips were mounted on to glass slides in mounting medium and stored at 4°C for imaging analysis. Primary antibodies include Guinea pig polyclonal anti-vGLUT1 antibody (1:500, Synaptic Systems, #135304), rabbit polyclonal anti-GABA antibody (1:500, Calbiochem, #PC213L), and mouse monoclonal anti-MAP2 (1:500, Sigma-Aldrich, Cat#M1406). Secondary antibodies include goat anti-mouse Alexa Flour488 antibody (1:500, Thermo Fisher Scientific, #A-11008), goat anti-guinea pig Alexa Fluor568 antibody (1:500, Thermo Fisher Scientific, #A-11075), and donkey anti-rabbit Alexa Flour647 antibody (1:500, Thermo Fisher Scientific, #A-31573).

Electrophysiology

Whole-cell patch-clamp recordings were performed using a Multiclamp 700B amplifier (Molecular Devices). The bath solution contained: 128 mM NaCl, 30 mM glucose, 5 mM KCl, 5 mM $CaCl_2$, 2 mM $MgCl_2$, and 25 mM HEPES (pH = 7.3, OSM:315–325). The patch pipettes were pulled from borosilicate glass (Sutter Instruments), and the resistance of pipettes filled with intracellular solution varied between 4 and 7 MΩ. For the EPSC recordings, GABA receptor antagonist picrotoxin (50 μM) and NMDAR antagonist AP5 (50 μM, Tocris) were applied to the bath solution, and pipette solution contained: 125 mM potassium gluconate, 10 mM KCl, 5 mM EGTA, 10 mM HEPES, 10 mM Tris–phosphocreatine, 4 mM MgATP, and 0.5 mM Na_2GTP (pH 7.3, OSM: 290). For the IPSC recordings, AMPAR antagonist CNQX (20 μM, Sigma) and NMDAR antagonist AP5 (50 μM, Tocris) were applied to the bath solution, and pipette solution contained: 147 mM CsCl, 5 mM Tris-phosphocreatine, 2 mM EGTA, 10 mM HEPES, 2 mM MgATP, and 0.3 mM Na_2GTP (pH = 7.3, OSM: 290). The membrane potential was held at –70 mV. To record evoked EPSCs, presynaptic neurons were stimulated with a theta-stimulating electrode, with a voltage step from 0 V to 20–30 V for 1 ms, to trigger an AP; evoked synaptic release was recorded from the postsynaptic neurons. The series resistance was typically <15 MΩ, and partially compensated to 60%–80%. For recordings of mEPSCs and mIPSCs, 0.5 μM tetrodotoxin (TTX, Tocris) was applied to the bath solution. Data were acquired and analyzed using pClampfit software (Molecular Devices), sampled at 10 kHz, and filtered at 2 kHz. Data are presented as mean ± SEM.

Immunoblotting

Neuron lysates were prepared with boiling lysis buffer (100 mM Tris–HCl, 200 mM DTT, 4% w/v SDS, 0.2% w/v bromophenol blue, 20% v/v glycerol, pH = 6.8). Proteins were separated by SDS–PAGE and blotted onto a polyvinylidene fluoride membrane (Millipore). Membranes were probed with the specific primary antibodies, followed by peroxidase-conjugated secondary antibodies. The bands were visualized by Chemiluminescence (Millipore). Antibodies used in this study include: SCGN (1:500, Santa Cruz, #sc374355), and tubulin (1:5000, Sigma, #T5076).

Cloning, protein expression, and purification

Expression and purification of human SCGN and SNAP-25 were described previously [42]. Briefly, SCGN and SNAP-25 were expressed with an N-terminal GST fusion. Protein expression was induced by the addition of 0.5 mM of isopropyl β-D-1-thiogalactopyranoside (IPTG) at 37°C for 4 h. Proteins were sequentially purified by GST affinity, anion exchange, and gel filtration chromatography on the Äkta Pure system (GE Healthcare). Full-length SNAP-25 was cloned into PET-28a-based expression vector with an N-terminal His_6 tag. The protein was purified on Ni-NTA affinity and Superdex 200 increase gel filtration chromatography (GE Healthcare). Human Doc2α and Doc2β were cloned into the PGEX 4T-1 vector, resulting in an N-terminal GST tag. The proteins were expressed at 18°C for 16 h after the addition of IPTG. GST-Doc2α or Doc2β was first captured by GST affinity resin. The GST fusion was then removed by on-column TEV cleavage, and eluted proteins were further purified by Superdex 75 increase gel filtration chromatography (GE Healthcare).

ITC

ITC experiments were performed at 25°C using ITC 200 (Microcal), as previously described [42]. SNAP-25-J or Doc2α C (200 or 140 μM) were titrated into the sample cell containing human SCGN (14 or 10 μM) in ITC buffer (20 mM Tris–HCl, 200 mM NaCl, pH = 8.0, 2 mM $CaCl_2$). Data were analyzed with the Origin 7.0 software package (OriginLab) by fitting the 'one set of sites' model.

GST pull-down assay

GST pull-down experiments were carried out as previously described [42]. Briefly, GST or GST-tagged proteins (20 μg) were incubated with 100 μg of bait protein. The proteins were mixed with glutathione sepharose 4B resin in 1 mL PB buffer (20 mM Tris–HCl, 200 mM NaCl, 2 mM $CaCl_2$ or 2 mM EDTA, 0.005% Triton X-100 or 0.5% Triton X-100, pH = 8.0). After washing with PB buffer 5 times, the bound proteins were separated by SDS–PAGE and visualized by Coomassie blue staining. Each experiment was repeated at least once and checked for consistency.

Research ethics

All experimental procedures were in full compliance with Tsinghua University's Guidelines for the Care and Use of Laboratory Animals. The experimental protocols were approved by the Animal Care and Use Committee at Tsinghua University (Ethics approval number: F16-00228; A5061-01).

Statistical analysis

Data are shown as mean values ± SEM. Two-tailed unpaired Student's *t*-test was used for all experiments. The analysis approaches have been justified as appropriate by previous biological studies, and all data met the criteria of normal distribution. The statistical data for all experiments are listed in Table S1. Statistical significance was evaluated at $P < 0.05$. Key resources are listed in Table S2.

Data availability

All data that supported the findings of this study are available within the article and its supplementary materials.

Supplementary data

Supplementary data is available at *Life Medicine* online.

Acknowledgements

We thank all members in the laboratory and Dr Haijia Yu (Nanjing Normal University) for helpful discussion and technical assistance. This work was supported by National Natural Science Foundation of China (NSFC) (No. 31830038 to J.Y.), Beijing Municipal Natural Science Foundation (No. Z210011 to J.Y.), NSFC (Nos. 32371008 to J.Y., 81901281 to Y.T.), and the Open Project of Collaborative Innovation Center for Language Ability of Jiangsu Province.

Author contributions

Y.T. conducted electrophysiological experiments. Q.M.Z. conducted immunostaining experiments. J.Q. conducted molecular biology and biochemistry experiments. T.S.T. and L.W. provided technical assistance. Y.T. analyzed the data. Y.T. and J.Y. designed the experiments and wrote the manuscript with inputs from all other authors.

Conflict of interest

The authors declare no competing interests.

References

1. Koh TW, Bellen HJ. Synaptotagmin I, a Ca^{2+} sensor for neurotransmitter release. *Trends Neurosci* 2003;26:413–22.
2. Sun J, Pang ZP, Qin D, et al. A dual-Ca^{2+}-sensor model for neurotransmitter release in a central synapse. *Nature* 2007;450:676–82.
3. Kaeser PS, Regehr WG. Molecular mechanisms for synchronous, asynchronous, and spontaneous neurotransmitter release. *Annu Rev Physiol* 2014;76:333–63.
4. Lau PM, Bi GQ. Synaptic mechanisms of persistent reverberatory activity in neuronal networks. *Proc Natl Acad Sci U S A* 2005;102:10333–8.
5. Iremonger KJ, Bains JS. Integration of asynchronously released quanta prolongs the postsynaptic spike window. *J Neurosci* 2007;27:6684–91.
6. Best AR, Regehr WG. Inhibitory regulation of electrically coupled neurons in the inferior olive is mediated by asynchronous release of GABA. *Neuron* 2009;62:555–65.
7. Yao J, Gaffaney JD, Kwon SE, et al. Doc2 is a Ca^{2+} sensor required for asynchronous neurotransmitter release. *Cell* 2011;147:666–77.
8. Deng S, Li J, He Q, et al. Regulation of recurrent inhibition by asynchronous glutamate release in neocortex. *Neuron* 2020;105:522–533.e4.
9. Carter AG, Regehr WG. Quantal events shape cerebellar interneuron firing. *Nat Neurosci* 2002;5:1309–18.
10. Sharma G, Vijayaraghavan S. Modulation of presynaptic store calcium induces release of glutamate and postsynaptic firing. *Neuron* 2003;38:929–39.
11. Sutton MA, Ito HT, Cressy P, et al. Miniature neurotransmission stabilizes synaptic function via tonic suppression of local dendritic protein synthesis. *Cell* 2006;125:785–99.
12. Sutton MA, Taylor AM, Ito HT, et al. Postsynaptic decoding of neural activity: eEF2 as a biochemical sensor coupling miniature synaptic transmission to local protein synthesis. *Neuron* 2007;55:648–61.
13. Sollner T, Bennett MK, Whiteheart SW, et al. A protein assembly-disassembly pathway *in-vitro* that may correspond to sequential steps of synaptic vesicle docking, activation, and fusion. *Cell* 1993;75:409–18.
14. Rizo J, Xu J. The synaptic vesicle release machinery. *Annu Rev Biophys* 2015;44:339–67.
15. Geppert M, Goda Y, Hammer RE, et al. Synaptotagmin I: a major Ca^{2+} sensor for transmitter release at a central synapse. *Cell* 1994;79:717–27.
16. Pang ZP, Melicoff E, Padgett D, et al. Synaptotagmin-2 is essential for survival and contributes to Ca^{2+} triggering of neurotransmitter release in central and neuromuscular synapses. *J Neurosci* 2006;26:13493–504.
17. Xu J, Mashimo T, Sudhof TC. Synaptotagmin-1, -2, and -9: Ca(2+) sensors for fast release that specify distinct presynaptic properties in subsets of neurons. *Neuron* 2007;54:567–81.
18. Bacaj T, Wu D, Yang X, et al. Synaptotagmin-1 and synaptotagmin-7 trigger synchronous and asynchronous phases of neurotransmitter release. *Neuron* 2013;80:947–59.
19. Xu J, Pang ZP, Shin O-H, et al. Synaptotagmin-1 functions as a Ca^{2+} sensor for spontaneous release. *Nat Neurosci* 2009;12:759–66.

20. Groffen AJ, Martens S, Díez Arazola R, et al. Doc2b is a high-affinity Ca^{2+} sensor for spontaneous neurotransmitter release. *Science* 2010;327:1614–8.
21. Orita S, Sasaki T, Naito A, et al. Doc2: a novel brain protein having two repeated C2-like domains. *Biochem Biophys Res Commun* 1995;206:439–48.
22. Sakaguchi G, Orita S, Maeda M, et al. Molecular cloning of an isoform of Doc2 having two C2-like domains. *Biochem Biophys Res Commun* 1995;217:1053–61.
23. Sugita S, Han W, Butz S, et al. Synaptotagmin VII as a plasma membrane Ca(2+) sensor in exocytosis. *Neuron* 2001;30:459–73.
24. Han W, Rhee J-S, Maximov A, et al. N-glycosylation is essential for vesicular targeting of synaptotagmin 1. *Neuron* 2004;41:85–99.
25. Kojima T, Fukuda M, Aruga J, et al. Calcium-dependent phospholipid binding to the C2A domain of a ubiquitous form of double C2 protein (Doc2 beta). *J Biochem* 1996;120:671–6.
26. Courtney NA, Briguglio JS, Bradberry MM, et al. Excitatory and inhibitory neurons utilize different Ca(2+) sensors and sources to regulate spontaneous release. *Neuron* 2018;98:977–991.e5.
27. Pang ZP, Bacaj T, Yang X, et al. Doc2 supports spontaneous synaptic transmission by a Ca(2+)-independent mechanism. *Neuron* 2011;70:244–51.
28. Wagner L, Oliyarnyk O, Gartner W, et al. Cloning and expression of secretagogin, a novel neuroendocrine- and pancreatic islet of Langerhans-specific Ca2+-binding protein. *J Biol Chem* 2000;275:24740–51.
29. Rogstam A, Linse S, Lindqvist A, et al. Binding of calcium ions and SNAP-25 to the hexa EF-hand protein secretagogin. *Biochem J* 2007;401:353–63.
30. Birkenkamp-Demtroder K, Wagner L, Brandt Sørensen F, et al. Secretagogin is a novel marker for neuroendocrine differentiation. *Neuroendocrinology* 2005;82:121–38.
31. Yang SY, Lee J-J, Lee J-H, et al. Secretagogin affects insulin secretion in pancreatic beta-cells by regulating actin dynamics and focal adhesion. *Biochem J* 2016;473:1791–803.
32. Malenczyk K, Girach F, Szodorai E, et al. A TRPV1-to-secretagogin regulatory axis controls pancreatic beta-cell survival by modulating protein turnover. *EMBO J* 2017;36:2107–25.
33. Mulder J, Zilberter M, Spence L, et al. Secretagogin is a Ca^{2+}-binding protein specifying subpopulations of telencephalic neurons. *Proc Natl Acad Sci U S A* 2009;106:22492–7.
34. Maj M, Milenkovic I, Bauer J, et al. Novel insights into the distribution and functional aspects of the calcium binding protein secretagogin from studies on rat brain and primary neuronal cell culture. *Front Mol Neurosci* 2012;5:84.
35. Krishnamurthy D, Harris LW, Levin Y, et al. Metabolic, hormonal and stress-related molecular changes in post-mortem pituitary glands from schizophrenia subjects. *World J Biol Psychiatry* 2013;14:478–89.
36. Deciphering Developmental Disorders, S. Large-scale discovery of novel genetic causes of developmental disorders. *Nature* 2015;519:223–8.
37. Romanov RA, Alpár A, Zhang M-D, et al. A secretagogin locus of the mammalian hypothalamus controls stress hormone release. *EMBO J* 2015;34:36–54.
38. Alhowikan AM, Ayadhi LA, Halepoto DM. Secretagogin (SCGN) plasma levels and their association with cognitive and social behavior in children with Autism Spectrum Disorder (ASD). *J Coll Physicians Surg Pak* 2017;27:222–6.
39. Sarkar A, Mei A, Paquola ACM, et al. Efficient generation of CA3 neurons from human pluripotent stem cells enables modeling of hippocampal connectivity in vitro. *Cell Stem Cell* 2018;22:684–697.e9.
40. Zahola P, Hanics J, Pintér A, et al. Secretagogin expression in the vertebrate brainstem with focus on the noradrenergic system and implications for Alzheimer's disease. *Brain Struct Funct* 2019;224:2061–78.
41. Hanics J, Szodorai E, Tortoriello G, et al. Secretagogin-dependent matrix metalloprotease-2 release from neurons regulates neuroblast migration. *Proc Natl Acad Sci U S A* 2017;114:E2006–15.
42. Qin J, Liu Q, Liu Z, et al. Structural and mechanistic insights into secretagogin-mediated exocytosis. *Proc Natl Acad Sci U S A* 2020;117:6559–70.
43. Wang QW, Qin J, Chen Y-F, et al. 16p112 CNV gene Doc2alpha functions in neurodevelopment and social behaviors through interaction with Secretagogin. *Cell Rep* 2023;42:112691.
44. Hagler DJ Jr, Goda Y. Properties of synchronous and asynchronous release during pulse train depression in cultured hippocampal neurons. *J Neurophysiol* 2001;85:2324–34.